LETTER

doi:10.1038/nature09779

Sensitivity to antitubulin chemotherapeutics is regulated by MCL1 and FBW7

Ingrid E. Wertz[1], Saritha Kusam[1], Cynthia Lam[1]*, Toru Okamoto[2]*, Wendy Sandoval[3], Daniel J. Anderson[4], Elizabeth Helgason[1], James A. Ernst[1,3], Mike Eby[4], Jinfeng Liu[5], Lisa D. Belmont[4], Joshua S. Kaminker[5], Karen M. O'Rourke[6], Kanan Pujara[7], Pawan Bir Kohli[8], Adam R. Johnson[8], Mark L. Chiu[9], Jennie R. Lill[3], Peter K. Jackson[4], Wayne J. Fairbrother[1], Somasekar Seshagiri[7], Mary J. C. Ludlam[4], Kevin G. Leong[4], Erin C. Dueber[1], Heather Maecker[4], David C. S. Huang[2,10] & Vishva M. Dixit[6]

Microtubules have pivotal roles in fundamental cellular processes and are targets of antitubulin chemotherapeutics[1]. Microtubule-targeted agents such as Taxol and vincristine are prescribed widely for various malignancies, including ovarian and breast adenocarcinomas, non-small-cell lung cancer, leukaemias and lymphomas[1]. These agents arrest cells in mitosis and subsequently induce cell death through poorly defined mechanisms[2]. The strategies that resistant tumour cells use to evade death induced by antitubulin agents are also unclear[2]. Here we show that the pro-survival protein MCL1 (ref. 3) is a crucial regulator of apoptosis triggered by antitubulin chemotherapeutics. During mitotic arrest, MCL1 protein levels decline markedly, through a post-translational mechanism, potentiating cell death. Phosphorylation of MCL1 directs its interaction with the tumour-suppressor protein FBW7, which is the substrate-binding component of a ubiquitin ligase complex. The polyubiquitylation of MCL1 then targets it for proteasomal degradation. The degradation of MCL1 was blocked in patient-derived tumour cells that lacked *FBW7* or had loss-of-function mutations in *FBW7*, conferring resistance to antitubulin agents and promoting chemotherapeutic-induced polyploidy. Additionally, primary tumour samples were enriched for *FBW7* inactivation and elevated MCL1 levels, underscoring the prominent roles of these proteins in oncogenesis. Our findings suggest that profiling the FBW7 and MCL1 status of tumours, in terms of protein levels, messenger RNA levels and genetic status, could be useful to predict the response of patients to antitubulin chemotherapeutics.

BCL2 family proteins are key regulators of cell survival and can either promote or inhibit cell death[3]. Pro-survival members, including BCL-X_L and MCL1, inhibit apoptosis by blocking the cell death mediators BAX and BAK (also known as BAK1). When uninhibited, BAX and BAK permeabilize the outer mitochondrial membranes, which releases pro-apoptotic factors that activate caspases, the proteases that catalyse cellular demise. This intrinsic, or mitochondrial, pathway is initiated by the damage-sensing BH3-only proteins, including BIM (encoded by *BCL2L11*) and NOXA (also known as PMAIP1), which neutralize the pro-survival family members when cells are irreparably damaged[4].

Because aberrant expression of pro-survival BCL2 family proteins promotes tumorigenesis and resistance to chemotherapeutics[3], we evaluated whether these proteins regulate the cell death induced by antitubulin agents. Multiple lineages of $Bax^{-/-}Bak^{-/-}$ mouse embryonic fibroblasts (MEFs) were resistant to killing by Taxol or nocodazole, whereas wild-type (WT) MEFs were significantly more sensitive to such killing (Fig. 1a and Supplementary Fig. 2a–e). These results were confirmed in myeloid cells (Fig. 1b). As inhibitor of apoptosis (IAP) proteins[5] do not have a significant role in the cellular response to antitubulin agents (Supplementary Fig. 3), we conclude that BCL2 family proteins are key regulators of antitubulin-agent-induced cell death in diverse cell types.

Next we determined the sensitivity of MEFs lacking individual BCL2 family members to killing by Taxol or vincristine, two mechanistically distinct antitubulin chemotherapeutics. $Bclx^{-/-}$ cells were more sensitive to Taxol than were WT cells, and $Mcl1^{-/-}$ cells showed greater sensitivity than WT cells to Taxol or vincristine (Fig. 1c, d). Because the ratio of pro-survival to pro-apoptotic BCL2 family proteins dictates cell fate[3], we monitored the levels of these proteins during mitotic arrest, as indicated by phosphorylation of the anaphase-promoting complex subunit CDC27 (ref. 6). MCL1 protein levels declined markedly in synchronized cells released into nocodazole or Taxol (Fig. 1e and Supplementary Fig. 4). The decrease in NOXA protein levels is probably an indirect consequence of MCL1-regulated stability (D.C.S.H., unpublished observations). MCL1 protein levels also declined in unsynchronized cells that were arrested in mitosis (Supplementary Figs 5 and 34).

MCL1 transcription was not significantly decreased during mitotic arrest in human cell lines (Fig. 2a). This implicated a role for the ubiquitin–proteasome system, the primary conduit for regulated protein degradation in eukaryotic cells[7], in the reduction of MCL1 protein levels. Indeed, the proteasome inhibitor MG132 blocked MCL1 degradation (Fig. 2b and Supplementary Fig. 6), and endogenous MCL1 was ubiquitylated during mitotic arrest (Supplementary Fig. 7).

MCL1 contains potential degron motifs for association with the F-box proteins β-transducin-repeat-containing protein (β-TRCP; also known as FBXW1 or FWD1)[8] and FBW7 (also known as FBXW7, AGO, CDC4 or SEL10)[9] (Supplementary Fig. 8). F-box proteins are substrate receptors for SKP1–CUL1–F-box (SCF)-type ubiquitin ligase complexes, which mediate degradative polyubiquitylation[9,10]. Consistent with a role for CUL1-based ubiquitin ligases in MCL1 turnover, ectopic expression of a dominant-negative CUL1 protein blocked MCL1 degradation during mitotic arrest (Supplementary Fig. 9). These data indicate that CUL1-containing ubiquitin-ligase complexes have a more prominent role in regulating MCL1 turnover during mitotic arrest than MULE, a ligase that ubiquitylates MCL1 (ref. 11), an idea corroborated by knocking down MULE expression in Taxol-treated cells by using RNA interference (RNAi) (Supplementary Fig. 10a–c). RNAi-mediated knockdown of FBW7 expression, but not β-TRCP expression, attenuated MCL1 degradation in tumour cells (Fig. 2c and Supplementary Figs 11 and 12) and untransformed cells (Supplementary Fig. 13a, b). MCL1 degradation (Fig. 2d) and turnover (Supplementary Fig. 14) was protracted in *FBW7*-null cells relative to

[1]Department of Early Discovery Biochemistry, Genentech, South San Francisco, California 94080, USA. [2]The Walter and Eliza Hall Institute of Medical Research, Parkville, Victoria 3052, Australia. [3]Department of Protein Chemistry, Genentech, South San Francisco, California 94080, USA. [4]Department of Research Oncology, Genentech, South San Francisco, California 94080, USA. [5]Department of Bioinformatics, Genentech, South San Francisco, California 94080, USA. [6]Department of Physiological Chemistry, Genentech, South San Francisco, California 94080, USA. [7]Department of Molecular Biology, Genentech, South San Francisco, California 94080, USA. [8]Department of Biochemical Pharmacology, Genentech, South San Francisco, California 94080, USA. [9]Department of Structural Biology, Abbott Laboratories, Abbott Park, Illinois 60064, USA. [10]Department of Medical Biology, University of Melbourne, Parkville, Victoria 3010, Australia.
*These authors contributed equally to this work.

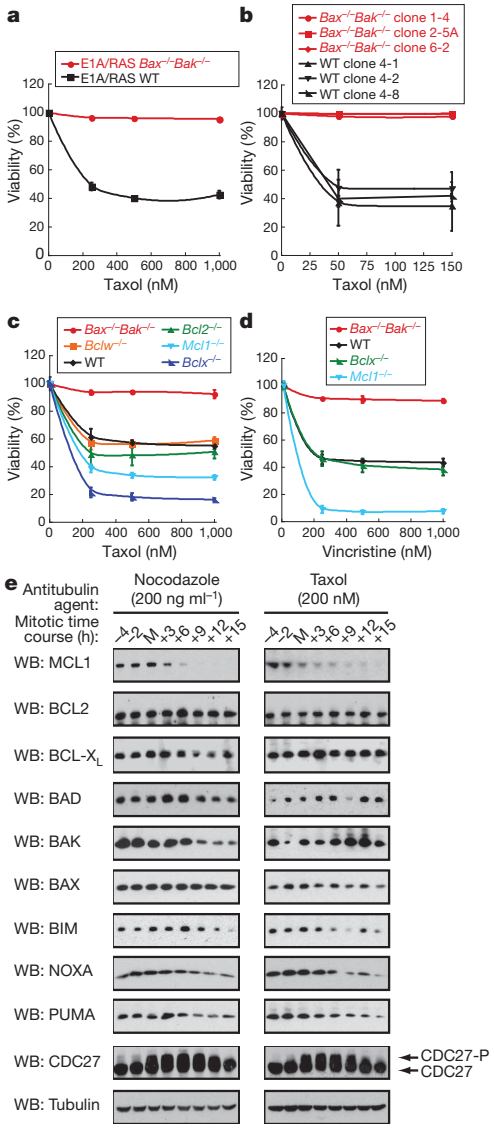

Figure 1 | BCL2 family proteins regulate cell death induced by antitubulin chemotherapeutic agents. **a**–**d**, Viability of cell lines treated for 48 h with the indicated agents. Data are presented as the mean ± s.e.m.; $n = 3$. E1A/RAS-transformed $Bax^{-/-}Bak^{-/-}$ MEFs (**a**) and factor-dependent myeloid (FDM) cells (**b**) are resistant to Taxol-induced cell death. **c**, Genetic deletion of *Mcl1* or *Bclx* enhances sensitivity to Taxol. **d**, Genetic deletion of *Mcl1*, but not of *Bclx*, enhances sensitivity to vincristine. **e**, Assessment of BCL2 family protein levels, by western blotting (WB), during mitotic arrest. The mitotic time course indicates when synchronized cells were collected relative to the onset of mitotic arrest: that is, −2 denotes 2 h before mitosis (M), and +3 denotes 3 h after cells entered mitosis. CDC27 and tubulin are indicators of mitotic arrest and equal loading, respectively. CDC27-P, phosphorylated CDC27.

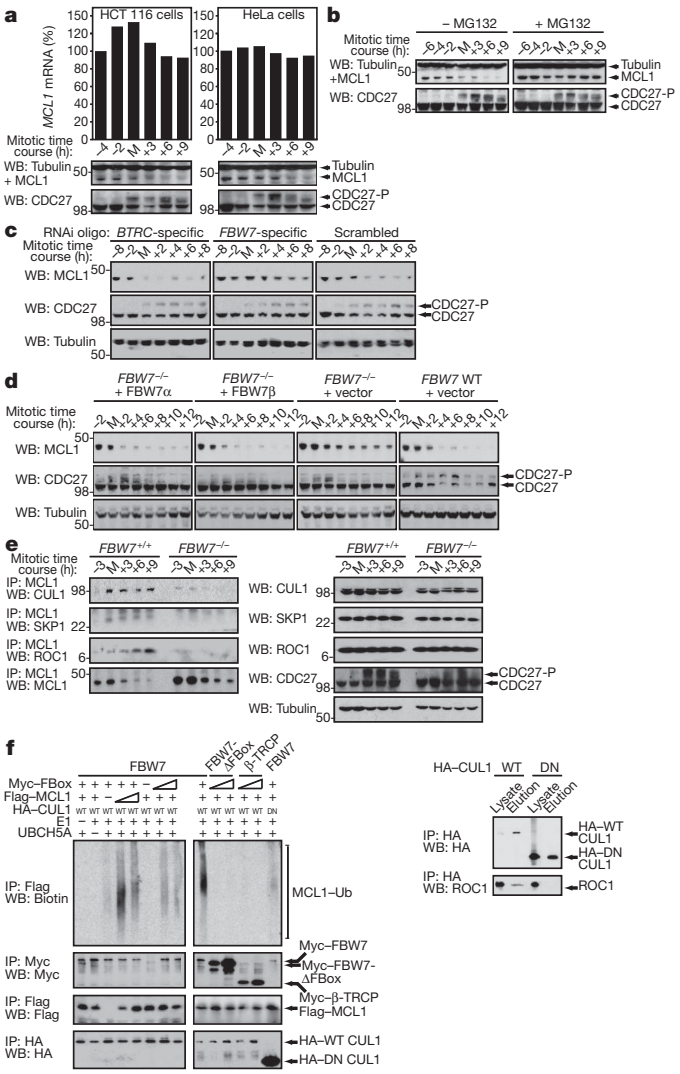

Figure 2 | SCF^{FBW7} targets MCL1 for proteasomal degradation during mitotic arrest. **a**–**e**, Human carcinoma cell lines were synchronized and collected throughout the mitotic time course as in Fig. 1a (numbers indicate molecular mass in kDa). **a**, During mitotic arrest, *MCL1* mRNA levels are not significantly decreased relative to MCL1 protein, as determined by WB. *MCL1* expression was monitored by real-time PCR, and the percentage mRNA is indicated relative to the −4-h time point. **b**, MG132 stabilizes MCL1 degradation during mitotic arrest in HeLa cells. **c**, RNAi oligonucleotides targeting *FBW7*, but not control scrambled RNAi or RNAi oligonucleotides targeting *BTRC* (which encodes β-TRCP), attenuate MCL1 degradation during mitotic arrest in HCT 116 cells. **d**, MCL1 degradation is attenuated in $FBW7^{-/-}$ HCT 116 cells during mitotic arrest. Complementation with the α-isoform or β-isoform of FBW7 restores MCL1 degradation. **e**, FBW7 recruits MCL1 to the SCF ubiquitin ligase complex core, the components of which are CUL1, SKP1 and ROC1, in HCT 116 cells in mitotic arrest. IP, immunoprecipitation. **f**, Left, reconstitution of the SCF^{FBW7} ubiquitin ligase complex promotes MCL1 ubiquitylation *in vitro*. Ubiquitylation reactions containing the indicated components were reacted *in vitro* with biotinylated ubiquitin. Reacted components were denatured, and Flag–MCL1 was immunoprecipitated (IP) and blotted (WB) for biotin to reveal *in vitro*-ubiquitylated MCL1 (MCL1–Ub). Myc-tagged F-box proteins (including F-box-deleted FBW7 (FBW7-ΔFBox)), Flag–MCL1 and HA-tagged CUL1 variants were also immunoprecipitated and analysed as indicated by WB analysis to reveal the respective input levels. Wedges indicate an increasing amount of the indicated reaction component. Right, endogenous ROC1 does not associate with dominant-negative (DN) HA-tagged CUL1. E1, ubiquitin-activating enzyme; UBCH5A, E2 ubiquitin-conjugating enzyme.

WT cells, and complementation with FBW7 isoforms restored MCL1 degradation (Fig. 2d and Supplementary Fig. 15). Endogenous MCL1 was recruited to cellular SCF complex subunits in *FBW7*-WT but not *FBW7*-null cells during mitotic arrest (Fig. 2e). Recombinant MCL1 was ubiquitylated *in vitro* by the reconstituted FBW7-containing SCF complex (SCF^{FBW7}) when the complete ligase complex was assembled (Fig. 2f). Collectively, these results demonstrate that SCF^{FBW7} promotes MCL1 degradation during mitotic arrest.

Because substrate phosphorylation promotes recruitment to FBW7 (ref. 9), the phosphorylation status of candidate FBW7-binding degrons on MCL1 was evaluated in cells arrested in mitosis (Fig. 3a). Mass spectrometry identified phosphorylation of residues S64, S121, S159 and T163 (Fig. 3a and Supplementary Fig. 16a–d). Myc-tagged MCL1

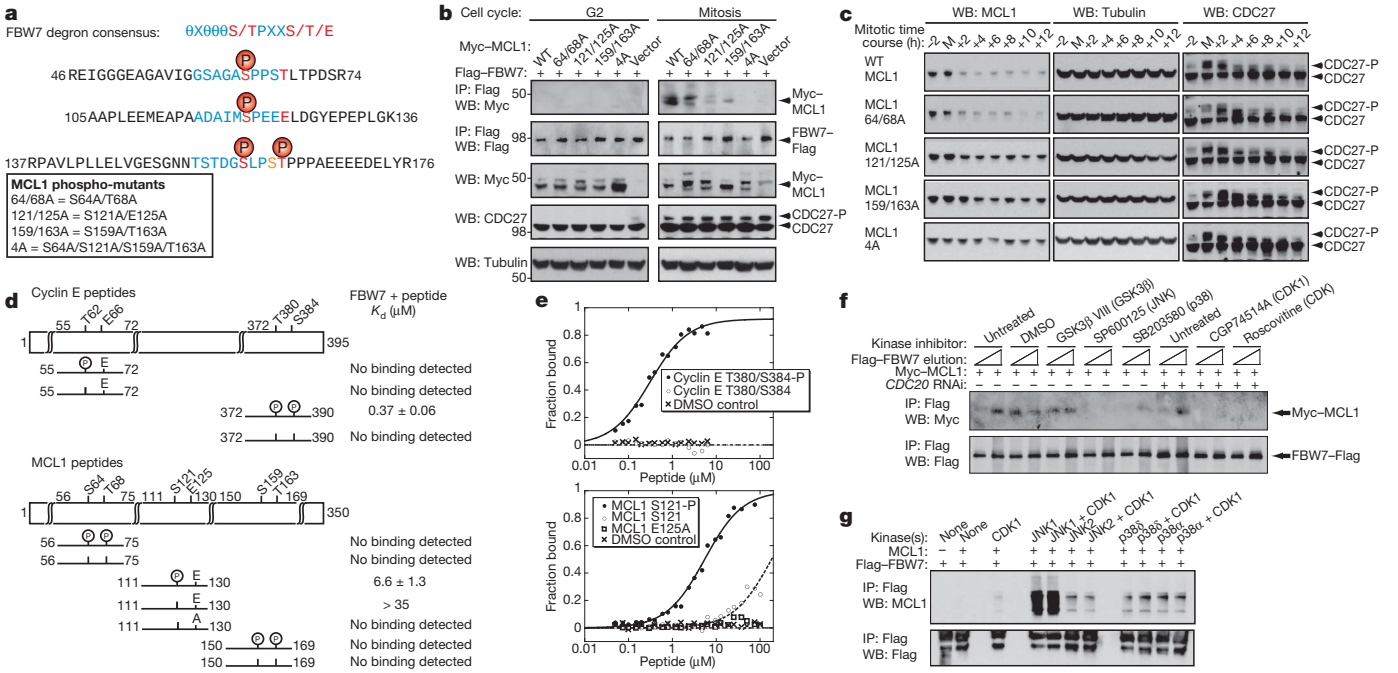

Figure 3 | Identification of MCL1 degron motifs and protein kinases that direct recruitment to FBW7 during mitotic arrest. **a**, The FBW7 degron consensus sequence (top, with potential phosphorylation sites or phospho-mimic residues in red), corresponding MCL1 residues (coloured, centre) and confirmed phosphorylation sites (P) during mitosis are indicated for three MCL1-derived peptide sequences. Phosphorylation at S159 (red) rather than S162 (orange) was confirmed by co-elution with a synthetic peptide (see Supplementary Fig. 16). θ, hydrophobic amino acid; X, any amino acid. The MCL1 phospho-mutant nomenclature used is indicated. **b**, Association of Flag–FBW7 with Myc–MCL1 mutants S121A/E125A, S159A/T163A, and 4A is attenuated in mitotic arrest. The indicated constructs were expressed in HeLa cells that were synchronized, released into Taxol, and processed as indicated. **c**, MCL1 phospho-mutants S121A/E125A, S159A/T163A and 4A have attenuated degradation during mitotic arrest. HCT 116 cells were synchronized and collected throughout the mitotic time course as in Fig. 1a. **d**, Schematic representation of MCL1- or cyclin-E-derived peptides and their calculated dissociation constants (K_d), averaged from duplicate experiments (mean ± s.d.), for FBW7 binding as determined by ELISA. **e**, The MCL1-derived peptide containing the phosphorylated S121/E125 degron (MCL1 S121-P) preferentially binds to FBW7 *in vitro*. Graphical representation of the fraction of FBW7-bound cyclin E or MCL1 peptides as a function of peptide concentration is shown. DMSO, dimethylsulphoxide. **f**, Pharmacological inhibition of JNK, p38 or CDK1 (with inhibitor (and targeted kinase) indicated, top) attenuates recruitment of Myc–MCL1 to Flag–FBW7 during mitotic arrest. The indicated constructs were expressed in HeLa cells with or without *CDC20* RNAi oligonucleotides or control scrambled RNAi oligonucleotides, and cells were then synchronized and released into Taxol. When cells entered mitotic arrest, the indicated agents were added for 1 h followed by a 3-h incubation with 25 μM MG132 before collection and processing as indicated (see Supplementary Fig. 25). **g**, *In vitro* phosphorylation of recombinant MCL1 drives FBW7 binding. Full-length MCL1 was subjected to *in vitro* phosphorylation with the indicated kinases and subsequently incubated with recombinant Flag–FBW7. Anti-Flag immunoprecipitates were resolved by SDS–PAGE and probed with antibodies specific for the indicated proteins.

was efficiently recruited to Flag-tagged FBW7 during mitotic arrest (Supplementary Fig. 17), and MCL1 residues 1–170 directed binding to FBW7 (Supplementary Fig. 18), thus mutant MCL1 constructs were tested to identify the degrons that confer FBW7 association (Fig. 3a). The MCL1 mutants S121A/E125A (in which the serine residue at position 121 and the glutamic acid residue at position 125 are both replaced by alanine residues) and S159A/T163A bound to FBW7 less efficiently than WT FBW7 (Fig. 3b), and their degradation during mitotic arrest was attenuated (Fig. 3c). Assessment of the relative affinities of the phosphorylated WT MCL1 degrons for FBW7 showed that the S121/E125 site is a higher affinity degron than the S159/T163 site (Fig. 3d, e). Thus, similar to other FBW7 substrates such as cyclin E[9], MCL1 contains high-affinity and low-affinity FBW7 degrons, both of which are required for efficient recruitment to (Fig. 3b) and subsequent degradation by (Fig. 3c) SCF^{FBW7} in the context of full-length MCL1.

To investigate the protein kinase or kinases that direct MCL1 recruitment to FBW7 in response to antitubulin chemotherapeutics, we focused on kinases that contain MCL1 degron consensus sites and demonstrate activity in mitotic arrest. This includes CDK1, casein kinase II (CKII), ERK isoforms (also known as MAPK1 and MAPK2), GSK3β, JNK isoforms (also known as MAPK8, MAPK9 and MAPK10) and p38 isoforms (also known as MAPK11, MAPK12, MAPK13 and MAPK14) (Supplementary Figs 19 and 24c). Studies using protein kinase inhibitors (Supplementary Figs 20a, 21, 22a, b and 24a, b) or RNAi (Supplementary Figs 20b, 23a–c and 24a–c) indicated that the activities of JNK, p38, CKII and CDK1 regulate MCL1 degradation during mitotic arrest. Because CDK1 inhibition drives cells out of mitosis[12] (Supplementary Figs 21 and 22a, b), non-degradable cyclin B1 was expressed, or *CDC20* expression was knocked down, to maintain cells in mitotic arrest[13] (Supplementary Fig. 24a, b). Inhibition of JNK, p38 or CDK1 also attenuated MCL1 recruitment to FBW7 (Fig. 3f and Supplementary Figs 25 and 26). JNK, p38 and CKII, but not CDK1, directly phosphorylated MCL1 degrons (Supplementary Table 1a–c). JNK and p38 directly promoted MCL1–FBW7 binding, whereas the contribution by CDK1 was negligible (Fig. 3g), suggesting that CDK1 indirectly enhances MCL1 phosphorylation to promote binding to FBW7 in the cellular context. Indeed, CDK1 phosphorylates T92 (Supplementary Table 1d), a residue that is phosphorylated (Supplementary Fig. 16e) and regulates MCL1 turnover (Supplementary Fig. 27a) during mitotic arrest.

Because the phosphatase inhibitor okadaic acid regulates MCL1 phosphorylation in a manner similar to Taxol[14], we evaluated whether CDK1-directed phosphorylation of T92 blocked the association of the okadaic-acid-sensitive phosphatase PP2A with MCL1 during mitotic arrest. PP2A more readily dissociated from WT MCL1 than the T92A mutant, concomitant with increasing CDK1 activity (Supplementary Fig. 27b). MCL1-associated PP2A protein levels and phosphatase activity are low in mitotic arrest when CDK1 activity is high, but they are restored after exit from mitosis, when CDK1 is inactivated (Supplementary Fig. 27c). Thus, the phosphorylation of MCL1 degron

residues by JNK, p38 and CKII during mitotic arrest is probably initially opposed by phosphatases such as PP2A. Maximal activation of CDK1 in prolonged mitotic arrest promotes T92 phosphorylation and PP2A dissociation, allowing sufficient phosphorylation of MCL1 degron residues to drive FBW7-mediated degradation (Supplementary Fig. 1). These effects are revealed when microtubule-targeted agents are washed out of cells that are in mitotic arrest: the activities of JNK, p38 and CDK1 decline, and MCL1 protein levels are restored (Supplementary Fig. 28). Sufficient loss of MCL1 activates BAK and BAX (Supplementary Fig. 29) to promote apoptosis.

FBW7 is a haploinsufficient tumour suppressor that targets proto-oncoproteins—including Myc, Jun, NOTCH and cyclin E—for degradation[9]. *FBW7* mutations that were identified in patient-derived cell lines disrupted the association of FBW7 with MCL1 during mitotic arrest (Supplementary Fig. 30). Thus, failure of inactivated FBW7 to promote MCL1 degradation could confer resistance to antitubulin chemotherapeutics. Indeed, *FBW7*-null cell lines showed attenuated MCL1 degradation and were more resistant to Taxol- or vincristine-induced cell death than were WT cells (Supplementary Figs 31 and 32). BCL-X_L remained stable regardless of *FBW7* status (Supplementary Fig. 31).

Similar trends were seen in patient-derived ovarian (Fig. 4a) and colon (Supplementary Fig. 33) cancer cell lines harbouring naturally occurring *FBW7* mutations. Although the response to antitubulin agents is heterogeneous within a cell population[15], mitotic arrest was similarly activated by Taxol treatment in synchronized and asynchronous ovarian cancer cell lines (Fig. 4a and Supplementary Fig. 34). Moreover, MCL1 degradation profiles were similar in synchronized and asynchronous cells: MCL1 was efficiently degraded in *FBW7*-WT cells that are effectively arrested in mitosis, yet MCL1 persisted in TOV21G cells that undergo only transient mitotic arrest and in *FBW7*-mutant SKOV3 cells (Fig. 4a and Supplementary Fig. 34). Thus, the inappropriate survival of cells that are arrested in mitosis positively correlates with attenuated MCL1 degradation, which is, in turn, regulated by FBW7.

FBW7 with an R505L mutation was expressed in *FBW7*-WT TOV112D-X1 cells to mimic cells harbouring one mutated *FBW7* allele[9] and to assess the *in vivo* effects. Tumours expressing mutant FBW7 were more resistant to Taxol (Supplementary Fig. 35a) and had higher levels of MCL1 than *FBW7*-WT parental tumours (Supplementary Fig. 35b, c). BCL-X_L protein levels were unaffected by *FBW7* status (Supplementary Fig. 35b, d). Reducing the amount of MCL1 protein in *FBW7*-null cells restored their sensitivity to Taxol- and vincristine-induced death (Fig. 4b and Supplementary Fig. 36), demonstrating that MCL1 is a crucial pro-survival factor that is responsible for resistance to antitubulin agents in FBW7-deficient cells.

Previous studies have shown that blocking apoptosis during mitotic arrest allows cells to exit mitosis and evade cell death[15] and that *FBW7*-null cells more frequently exit mitosis and undergo endoreduplication to render cells polyploid[16]. Our work identifying MCL1 as an FBW7 substrate therefore suggests a molecular link to explain antitubulin agent resistance and chemotherapy-induced polyploidy. Indeed, *FBW7*-null cells exit Taxol- or vincristine-induced mitotic arrest more readily (Fig. 4d and Supplementary Figs 37 and 38) and show more pronounced polyploidy (Fig. 4c) than do *FBW7*-WT cells. Reducing the MCL1 protein levels in the *FBW7*-null cells with short hairpin RNA (shRNA) decreased mitotic slippage, enhanced Taxol- or vincristine-induced apoptosis (Fig. 4d and Supplementary Figs 37 and 38) and reduced chemotherapeutic-induced polyploidy (Fig. 4c) compared with *FBW7*-null cells treated with control shRNA. Thus, MCL1 promotes resistance to death induced by antitubulin chemotherapeutics and facilitates genomic instability when *FBW7* is inactivated.

The hostile tumour micro-environment, like chemotherapeutic insults, exerts selective pressures on malignant cells; therefore, tumour

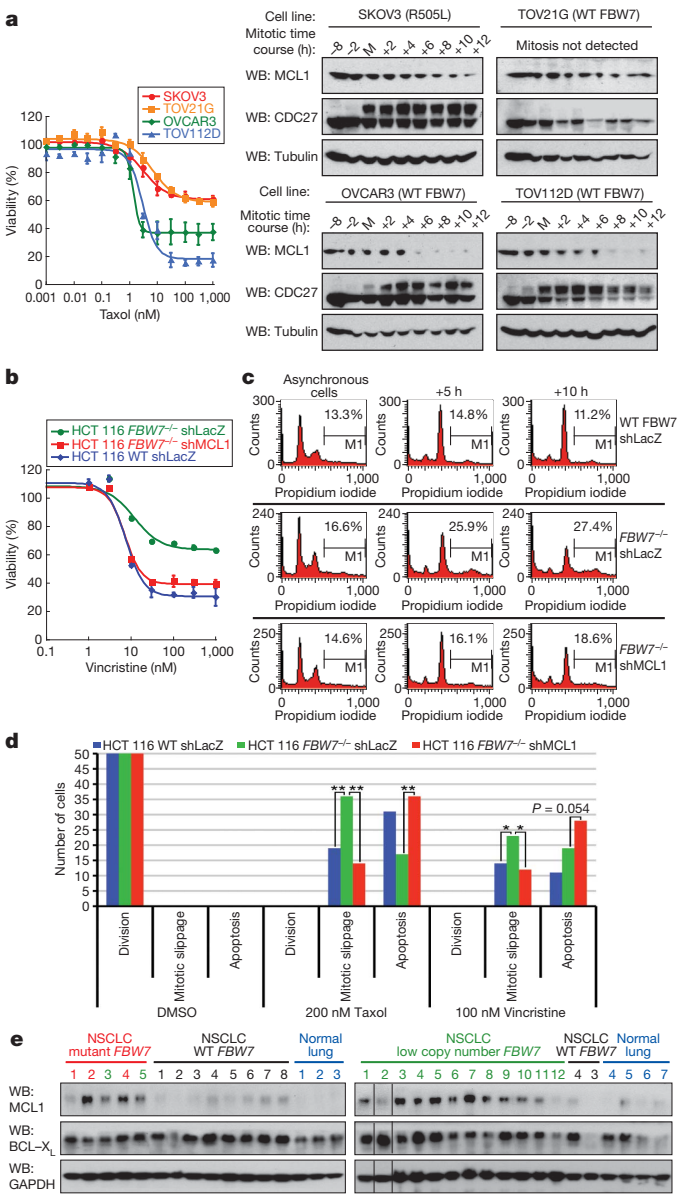

Figure 4 | *FBW7* inactivation and increased MCL1 levels promote antitubulin agent resistance and tumorigenesis in human cancers. a, *FBW7*-WT ovarian cancer cell lines that undergo mitotic arrest are sensitive to Taxol (left) and rapidly degrade MCL1 relative to FBW7-mutant and Taxol-resistant cells (right). *FBW7* status is specified in parentheses. **b**, Sensitivity to vincristine-induced cell death is restored in $FBW7^{-/-}$ cells on MCL1 ablation (red). WT or $FBW7^{-/-}$ HCT 116 cells were transduced with the indicated doxycycline-inducible shRNA constructs, cultured in the presence of doxycycline, and treated with various concentrations of vincristine for 48 h before cell viability assessment. shLacZ, control shRNA (green and blue). Data are presented as mean ± s.e.m.; $n = 3$. **c**, MCL1 expression modulates polyploidy in FBW7-deficient HCT 116 cells. WT or $FBW7^{-/-}$ HCT 116 cells were transduced with the indicated doxycycline-inducible shRNA constructs, cultured in the presence of doxycycline, synchronized and released into vincristine. They were then collected at 5 h (+5 h) or 10 h (+10 h) after mitotic arrest and fixed, stained with propidium iodide and analysed by FACS (*x* axis, fluorescence units; *y* axis, number of cells). M1, percentage of cells with >2*N* DNA content. **d**, MCL1 expression increases mitotic slippage and attenuates apoptosis in FBW7-deficient cells. WT or $FBW7^{-/-}$ HCT 116 cells were transduced with the indicated doxycycline-inducible shRNA constructs, cultured in the presence of doxycycline, transduced with an H2B–GFP-expressing baculovirus, synchronized, treated with the indicated antitubulin agents and imaged live. Three images were acquired every 10 min for 43 h, and 50 cells were analysed for each condition. *, $P < 0.05$; **, $P < 0.001$ (one-tailed Fisher's exact test). **e**, MCL1 levels are elevated in non-small-cell lung cancer (NSCLC) samples with mutant *FBW7* or low *FBW7* copy number relative to *FBW7*-WT tumours and normal lung samples (see also Supplementary Table 2). NSCLC *FBW7*-mutant samples 3 and 5 (green) also have low *FBW7* copy number.

cells harbouring alterations in FBW7 and MCL1 should be selected for and enriched in primary patient tumour samples. To this end, copy number analysis of *FBW7* and *MCL1* was performed in ovarian tumour samples (Supplementary Fig. 39). The co-occurrence of *MCL1* gain and *FBW7* loss was more frequent than expected, a finding that is consistent with selection for both genetic alterations (Supplementary Fig. 39). Data from non-small-cell lung cancer samples showed similar trends but were not statistically significant owing to insufficient sample size (data not shown). Immunoblotting of patient samples revealed that most tumours in which *FBW7* was inactivated had increased MCL1 protein levels relative to *FBW7*-WT tumours and normal lung samples (Fig. 4e and Supplementary Table 2). By contrast, BCL-X_L protein levels were not correlated with *FBW7* status (Fig. 4e). Thus, functional FBW7 is required to downregulate MCL1 expression in primary patient samples, a particularly significant finding given that antitubulin agents are therapeutic mainstays for non-small-cell lung cancers and ovarian cancers.

The signalling pathways that activate cell death induced by antitubulin chemotherapeutics are of crucial interest, and we provide genetic evidence that both *MCL1* and *BCLX* are important regulators of this therapeutic response. Whereas BCL-X_L is functionally inactivated by phosphorylation[17] and is unaffected by FBW7 status, MCL1 inactivation is coordinated by the concerted activities of phosphatases, stress-activated and mitotic kinases, and the SCF^{FBW7} ubiquitin ligase. As such, we define a unique molecular mechanism for regulation of MCL1 and initiation of apoptosis during mitotic arrest (Supplementary Fig. 1). By identifying SCF^{FBW7} as a crucial ubiquitin ligase that directs MCL1 degradation during mitotic arrest, we also elucidate a mechanism for resistance to antitubulin chemotherapeutics. Analysis of patient samples suggests that drug-efflux pumps[18] or tubulin alterations[19] do not always account for resistance to antitubulin agents, thus evasion of apoptosis owing to inappropriately increased levels of MCL1 is probably a crucial strategy. We also show that the elevated MCL1 protein levels in FBW7-deficient cells favours increased mitotic slippage, endoreduplication and subsequent polyploidy in response to antitubulin therapeutics. The role of MCL1 in FBW7-deficient cells therefore extends beyond the simple inhibition of apoptosis; it also facilitates genomic aberrations, thus fuelling the transformed state.

METHODS SUMMARY

The viability of cancer cell lines, and MEFs in which genes encoding IAPs had been knocked out, was analysed by using the CellTiter-Glo Luminescent Cell Viability Assay (Promega). Cells were treated in triplicate with antitubulin agents for the indicated times, using dimethylsulphoxide treatment as a control. The viability of BCL2-family-member-null MEFs was analysed by propidium iodide staining, as described previously[20], after treatment with antitubulin agents for 48 h. Cell synchronization was achieved by culture either in serum-free medium for 12–16 h or in medium containing 2 mM thymidine for 18–24 h, release from the thymidine block with three washes in PBS, followed by culture for 8–12 h in complete growth media (compositions are described in the Supplementary Information). Cells then underwent a second thymidine block for 16–20 h, three further washes in PBS and release into complete medium containing the indicated reagents. To block MCL1 degradation, 25 μM MG132 was added as cells entered mitotic arrest, as assessed by visual inspection. See Supplementary Information for full methods.

Received 13 October 2009; accepted 21 December 2010.

1. Jackson, J. R., Patrick, D. R., Dar, M. M. & Huang, P. S. Targeted anti-mitotic therapies: can we improve on tubulin agents? *Nature Rev. Cancer* **7,** 107–117 (2007).
2. Rieder, C. L. & Maiato, H. Stuck in division or passing through: what happens when cells cannot satisfy the spindle assembly checkpoint. *Dev. Cell* **7,** 637–651 (2004).
3. Youle, R. J. & Strasser, A. The BCL-2 protein family: opposing activities that mediate cell death. *Nature Rev. Mol. Cell Biol.* **9,** 47–59 (2008).
4. Willis, S. N. *et al.* Apoptosis initiated when BH3 ligands engage multiple Bcl-2 homologs, not Bax or Bak. *Science* **315,** 856–859 (2007).
5. Varfolomeev, E. & Vucic, D. (Un)expected roles of c-IAPs in apoptotic and NFκB signaling pathways. *Cell Cycle* **7,** 1511–1521 (2008).
6. King, R. W. *et al.* A 20S complex containing CDC27 and CDC16 catalyzes the mitosis-specific conjugation of ubiquitin to cyclin B. *Cell* **81,** 279–288 (1995).
7. Finley, D. Recognition and processing of ubiquitin–protein conjugates by the proteasome. *Annu. Rev. Biochem.* **78,** 477–513 (2009).
8. Frescas, D. & Pagano, M. Deregulated proteolysis by the F-box proteins SKP2 and β-TrCP: tipping the scales of cancer. *Nature Rev. Cancer* **8,** 438–449 (2008).
9. Welcker, M. & Clurman, B. E. FBW7 ubiquitin ligase: a tumour suppressor at the crossroads of cell division, growth and differentiation. *Nature Rev. Cancer* **8,** 83–93 (2008).
10. Deshaies, R. J. & Joazeiro, C. A. RING domain E3 ubiquitin ligases. *Annu. Rev. Biochem.* **78,** 399–434 (2009).
11. Zhong, Q., Gao, W., Du, F. & Wang, X. Mule/ARF-BP1, a BH3-only E3 ubiquitin ligase, catalyzes the polyubiquitination of Mcl-1 and regulates apoptosis. *Cell* **121,** 1085–1095 (2005).
12. Potapova, T. A. *et al.* The reversibility of mitotic exit in vertebrate cells. *Nature* **440,** 954–958 (2006).
13. Huang, H. C., Shi, J., Orth, J. D. & Mitchison, T. J. Evidence that mitotic exit is a better cancer therapeutic target than spindle assembly. *Cancer Cell* **16,** 347–358 (2009).
14. Domina, A. M., Vrana, J. A., Gregory, M. A., Hann, S. R. & Craig, R. W. MCL1 is phosphorylated in the PEST region and stabilized upon ERK activation in viable cells, and at additional sites with cytotoxic okadaic acid or Taxol. *Oncogene* **23,** 5301–5315 (2004).
15. Gascoigne, K. E. & Taylor, S. S. Cancer cells display profound intra- and interline variation following prolonged exposure to antimitotic drugs. *Cancer Cell* **14,** 111–122 (2008).
16. Finkin, S., Aylon, Y., Anzi, S., Oren, M. & Shaulian, E. Fbw7 regulates the activity of endoreduplication mediators and the p53 pathway to prevent drug-induced polyploidy. *Oncogene* **27,** 4411–4421 (2008).
17. Terrano, D. T., Upreti, M. & Chambers, T. C. Cyclin-dependent kinase 1-mediated Bcl-x_L/Bcl-2 phosphorylation acts as a functional link coupling mitotic arrest and apoptosis. *Mol. Cell. Biol.* **30,** 640–656 (2010).
18. Ozalp, S. S., Yalcin, O. T., Tanir, M., Kabukcuoglu, S. & Etiz, E. Multidrug resistance gene-1 (*Pgp*) expression in epithelial ovarian malignancies. *Eur. J. Gynaecol. Oncol.* **23,** 337–340 (2002).
19. Mesquita, B. *et al.* No significant role for β tubulin mutations and mismatch repair defects in ovarian cancer resistance to paclitaxel/cisplatin. *BMC Cancer* **5,** 101 (2005).
20. Chen, L. *et al.* Differential targeting of prosurvival Bcl-2 proteins by their BH3-only ligands allows complementary apoptotic function. *Mol. Cell* **17,** 393–403 (2005).

Supplementary Information is linked to the online version of the paper at www.nature.com/nature.

Acknowledgements We thank P. Ekert for FDM cell lines, J. Stinson for sequencing assistance, S. Johnson and C. Santos for assistance with obtaining patient samples, P. Haverty for bioinformatics analysis, C. Grimaldi for cloning assistance, J. Dynek for TaqMan advice, D. French for tumour analysis, C. Quan and J. Tom for peptide synthesis, I. Zilberleyb and the Baculovirus Expression Group for cloning and protein production, S. Charuvu for generating MCL1 point mutants, A. Bruce for graphics assistance, the Genentech Cancer Genome Project Team, Z. Modrusan, R. Soriano and the microarray lab for ovarian tumour data sets, K. Newton for editorial assistance, W. Wei for sharing unpublished results, and A. Eldridge, D. Kirkpatrick, D. Vucic, E. Varfolomeev, T. Goncharov, A. Cochran, O. Huang, A. Huang, Y. Pereg, A. Loktev, D. Phillips, J. Wu, M. van Delft, D. Eaton, E. Shaulian, T. Hunter, S. Cory, J. Adams, A. Strasser, R. Deshaies and G. Evan for discussions. Work in the Huang laboratory is supported by the National Health and Medical Research Council (program grant #461221, IRIISS grant #361646 and a fellowship to D.C.S.H.), the Leukemia and Lymphoma Society (SCOR 7413), the National Institutes of Health (grants CA043540 and CA80188), the Australian Cancer Research Foundation, and an Australian Research Council Australian Postdoctoral fellowship to T.O. We apologize to our colleagues whose primary work could not be cited owing to space constraints.

Author Contributions I.E.W., S.K., T.O., J.A.E., P.B.K., A.R.J., C.L., E.C.D., E.H., H.M. and K.G.L. designed and performed *in vitro*, cell-based and *in vivo* experiments. D.J.A. and M.J.C.L. designed and performed microscopy experiments. S.K., C.L., K.M.O., M.L.C. and M.E. made constructs. J.L. and J.K. performed bioinformatics analysis, K.P. and S.S. provided sequencing analysis. W.S. and J.R.L. designed and performed mass spectrometry experiments. I.E.W., S.K., C.L., T.O., W.S., D.J.A., M.J.C.L., K.G.L., E.C.D., H.M. and V.M.D. prepared the manuscript and figures. W.S., L.D.B., P.K.J., W.J.F., D.J.A., P.B.K., A.R.J., M.J.C.L., H.M., D.C.S.H. and I.E.W. contributed to the study design and data analysis.

Author Information Reprints and permissions information is available at www.nature.com/reprints. The authors declare no competing financial interests. Readers are welcome to comment on the online version of this article at www.nature.com/nature. Correspondence and requests for materials should be addressed to I.E.W. (ingrid@gene.com).